Astronomy & Astrophysics manuscript no. output
December 1, 2024

Constraints on the X-ray-to-radio fluence ratio of FRB 20240114A

F. Eppel[1,2], M. Krumpe[3], P. Limaye[2], N. Intrarat[4], J. Wongphechauxsorn[1,2], M. Cruces[5,6,2,7,8], W. Herrmann[9], F. Jankowski[10], P. Jaroenjittichai[4], L. G. Spitler[2], and M. Kadler[1]

[1] Julius-Maximilians-Universität Würzburg, Institut für Theoretische Physik und Astrophysik, Lehrstuhl für Astronomie, Emil-Fischer-Straße 31, D-97074 Würzburg, Germany
e-mail: florian.eppel@uni-wuerzburg.de
[2] Max-Planck-Institut für Radioastronomie, Auf dem Hügel 69, D-53121 Bonn, Germany
[3] Leibniz-Institut für Astrophysik Potsdam (AIP), An der Sternwarte 16, D-14482 Potsdam, Germany
[4] National Astronomical Research Institute of Thailand, Chiang Mai, Thailand
[5] European Southern Observatory, Karl-Schwarzschild-Str. 2, D-85748 Garching bei München, Germany
[6] Joint ALMA Observatory, Alonso de Córdova 3107, Vitacura, Santiago, Chile
[7] Centre of Astro-Engineering, Pontificia Universidad Catolica de Chile, Av. Vicuna Mackenna 4860, Santiago, Chile
[8] Department of Electrical Engineering, Pontificia Universidad Catolica de Chile, Av. Vicuna Mackenna 4860, Santiago, Chile
[9] Astropeiler Stockert e.V., Astropeiler 2-4, D-53902 Bad Münstereifel, Germany
[10] LPC2E, OSUC, Univ Orleans, CNRS, CNES, Observatoire de Paris, F-45071 Orleans, France

Received Dec 1, 2024; accepted XXX

ABSTRACT

We report on multi-wavelength observations of FRB 20240114A, a nearby (z=0.13), hyperactive, repeating Fast Radio Burst, which was discovered in January 2024. We performed simultaneous observations of the source with the Effelsberg 100-m radio telescope, the Thai National Radio Telescope, the Astropeiler Stockert and the X-ray satellite XMM-Newton in May 2024. On 23 May 2024 we detected 459 bursts from the source using the Ultra Broad Band (UBB) receiver of the Effelsberg telescope, covering a frequency range from 1.3 ~~GHz~~ to 6 GHz. All bursts have simultaneous X-ray coverage by *XMM-Newton*, but no significant X-ray emission was found at the position of the FRB. In this publication, we present constraints on the X-ray-to-radio fluence ratio $\eta_{x/r}$ for the three brightest bursts detected in the campaign. The brightest burst exhibits a radio fluence of 2.6×10^{-17} erg cm^{-2}, while the 3σ upper limit to the 0.2−12 keV X-ray burst fluence lies in the range 3.4×10^{-11} erg cm^{-2} to 1.7×10^{-10} erg cm^{-2}, depending on the assumed spectral model. Assuming a conservative 10 keV black-body spectrum, the X-ray-to-radio fluence ratio can be constrained to $\eta_{x/r} < 6.5 \times 10^6$. A more realistic spectrum ~~can be estimated~~ using a cutoff power law model ($\Gamma = 1.56$, cutoff 84 keV) based on the Galactic magnetar SGR 1935+2154, which has previously shown X-ray bursts associated with FRB-like radio bursts. In this scenario, we find $\eta_{x/r} < 1.3 \times 10^6$. Regardless of the assumed spectral model, our constraints on $\eta_{x/r}$ are the most stringent reported for an individual extragalactic FRB to date. Our results are consistent with FRB 20240114A being powered by a similar mechanism as the Galactic magnetar SGR 1935+2154, which exhibited an X-ray-to-radio fluence ratio of $\eta_{x/r} \sim 2.5 \times 10^5$ (1−250 keV). We show that future multi-wavelength campaigns will be able to probe this limit if very bright radio bursts are detected with simultaneous X-ray coverage.

Key words. X-rays: bursts - Methods: observational - Stars: magnetars

1. Introduction

The origin of Fast Radio Bursts (FRBs) is still unclear and a plethora of theoretical models has been suggested to explain these bright pulses of radio emission with millisecond duration (Platts et al. 2019). Several of the proposed models predict associated multi-wavelength emission, but previous searches for X-ray or γ-ray counterparts of FRBs did not lead to any detection (Scholz et al. 2016, 2017, 2020; Pilia et al. 2020; Piro et al. 2021; Trudu et al. 2023; Pearlman et al. 2023; Yan et al. 2024; Cook et al. 2024). In early 2020, X-ray telescopes succeeded in detecting a ~~coincident~~ high-energy transient signal with an FRB-like burst (Tavani et al. 2021; Mereghetti et al. 2020; Bochenek et al. 2020; Li et al. 2021). The source of this signal was identified as the Galactic magnetar SGR 1935+2154, which exhibited several more simultaneous radio/X-ray flares (e.g., Ridnaia et al. 2021). This discovery showed for the first time that a magnetar can produce X-ray bursts in coincidence with FRB-like radio bursts as ~~indeed~~ had been predicted before (e.g., Metzger et al. 2019). It further suggests that coordinated radio and X-ray observations of FRBs may be able to detect coincident signals from other bright magnetar flares also in nearby extragalactic systems. On 26 Jan 2024, the CHIME/FRB collaboration reported the discovery of the new repeating Fast Radio Burst FRB 20240114A (Shin & CHIME/FRB Collaboration 2024). ~~Multiple~~ follow-up observations throughout the following weeks found very bright bursts (Ould-Boukattine et al. 2024b; Pelliciari et al. 2024; Panda et al. 2024; Kumar et al. 2024; Zhang et al. 2024b), burst storms of several hundred burst (Zhang et al. 2024a; Uttarkar et al. 2024; Ould-Boukattine et al. 2024a), and also high-frequency radio detections up to 6 GHz (Joshi et al. 2024; Hewitt et al. 2024; Limaye & Spitler 2024). FRB 20240114A was localized to the dwarf star-forming galaxy SDSS J212739.84+041945.8 with sub-arcsecond precision (Tian et al. 2024; Snelders et al. 2024) which lies at a redshift of $z = 0.130 \pm 0.002$ (Bhardwaj et al. 2024).

Motivated by the high-fluence bursts, hyperactivity and possibly associated X-ray emission, we obtained target-of-

opportunity observations of FRB 20240114A with the *XMM-Newton* X-ray satellite using Director's Discretionary Time (DDT). Additionally, we obtained simultaneous DDT radio observations with the Effelsberg 100-m telescope, the Thai National Radio Telescope (TNRT) and the Stockert Astropeiler. Here, we present first results from this multi-wavelength campaign. In section 2, we give an overview of the observations and analysis for all telescopes, in section 3 we present the results for the three brightest bursts detected in the campaign and in section 4 we discuss our findings in the broader context of FRB multi-wavelength studies.

2. Observations & analysis

The simultaneous X-ray and radio observations were split into three sessions. Two sessions were carried out with simultaneous observations by Stockert & *XMM-Newton* (17 May 2024 & 27 May 2024), one session (23 May 2024) included TNRT, Effelsberg, Stockert & *XMM-Newton*. An overview of the observing times on 23 May 2024 is shown in Fig. 1. Below, we provide an overview about the observing setups and general analysis steps performed for the individual telescopes.

2.1. Effelsberg 100-m Telescope

We observed FRB 20240114A with the Effelsberg 100-m telescope on 23 May 2024 for ~7 hours using the Ultra-Broad-Band (UBB) receiver, which covers a frequency range of 1.3−6 GHz. The data were recorded using the Effelsberg Direct Digitisation (EDD) backend (Barr et al. 2023) with a channel width of 0.5 MHz and time resolution of 0.128 ms. The data were recorded in five different sub-bands (band 1: 1.3−1.9 GHz, band 2: 1.9−2.6 GHz, band 3: 3.0−4.1 GHz, band 4: 4.1−5.2 GHz, band 5: 5.2−6.0 GHz). We searched the data for single bursts using `TransientX` (Men & Barr 2024) separately in every sub-band and found 459 unique bursts that could be identified as FRBs matched across sub-bands. In this publication we focus on the three brightest bursts that were detected with S/N > 100 (labelled B1, B2 and B3). In case of a constant X-ray-to-radio fluence ratio $\eta_{x/r}$, those are the best candidates to exhibit associated X-ray emission. For a detailed overview about the analysis of the UBB data we refer to Appendix A.

2.2. Stockert Telescope

The Astropeiler Stockert is a 25-m dish operated in L-band. The system equivalent flux density (SEFD) of the instrument is 385 Jy. Data was recorded as total-intensity 32-bit data with 98 MHz bandwidth (1332.25 MHz to 1430.5 MHz) and a time resolution of 218.45 μs using a fast Fourier transform backend (Barr et al. 2013). We searched for radio bursts using `prepsubband` and `single_pulse_search` from `PRESTO` (Ransom 2011). The threshold for single pulses was set to a signal to noise ratio of 7, corresponding to a completeness limit of ~ 14 Jy ms. Furthermore, data were filtered for RFI from nearby radar systems by applying the modulation index technique described by (Spitler et al. 2012) and then classified using `FETCH` (Agarwal et al. 2020; Agarwal & Aggarwal 2020). The bursts flagged by `FETCH` as potential candidates were manually inspected. During the time of the observation reported here, no burst was detected. An additional manual inspection of the data was performed around the arrival time of burst B1 with no convincing result. It has to be noted that at observation days other than reported here, bright burst (i.e., > *XX* Jy ms) from FRB 2024011A were detected ~~by the Stockert telescope~~ using the analysis described above.

2.3. Thai National Radio Telescope

The TNRT is a 40-m radio dish located at Doi Saket, Chiang Mai, Thailand, equipped with an EDD backend[1]. We performed pulsar search mode observations of FRB 20240114A on 23 May 2024 for ~ 7 hours (see Fig. 1), using the L-band receiver centered at 1350 MHz with a bandwidth of 900 MHz, and time resolution of 51.2 μs. We used `TransientX` (Men & Barr 2024) to search for single-pulses with DM between 510 and 570 cm^{-3} pc. The S/N cutoff was set to 7 and pulse width < 30 ms. After inspecting all candidates ~~manually~~, no burst has been found. This is consistent with the expected burst rate of 0.1 to 0.3 bursts/hour, assuming a conservative SEFD of 90 Jy (Jaroenjittichai et al. 2022).

2.4. XMM-Newton

We obtained *XMM-Newton* DDT observations which were carried out in three different time slots on 17 May 2024 (Obs.ID 0935190601, 25.2 ks total observing time), 23 May 2024 (Obs.ID 0935190701, 25 ks) and 27 May 2024 (0935191001, 28.7 ks). We used the PN- and MOS-instruments with medium filter in small window mode to achieve the best timing accuracy while also having good spatial resolution.

The data for the PN- and MOS-instruments were processed using the *XMM-Newton* Science Analysis System (`SAS`, Gabriel et al. 2004) version 21.0.0. We used the pipelines `epproc` for the PN-camera and `emproc` for the MOS-cameras to generate filtered event lists. We performed the barycentric correction using the `barycen` task. Additionally, for the calculation of a persistent unabsorbed flux limit at the position of FRB 20240114A, we identified times of flaring background by analyzing the light curves at low energies (i.e., 0.1−0.5 keV) and high energies (i.e., 10−15 keV). By applying conservative cuts to the background count rate, we identified the final good-time-intervals (GTIs) to use for the analysis of the persistent flux limit, totaling 57.3 ks. The event lists used for our analysis were extracted in the energy band 0.2−12 keV. Additionally, we performed an astrometric pointing correction using the `eposcorr` task (see Appendix B).

3. Results

3.1. Radio bursts

During the Effelsberg observation on 23 May 2024, we detected 459 bursts from FRB 20240114A using the UBB receiver. None of these bursts were seen by TNRT or Stockert, most likely due to their limited sensitivity as compared to Effelsberg. In the additional two XMM-Newton sessions that were covered only by Stockert, no bursts were found. In this work, we present the three brightest bursts (labelled B1, B2 and B3) detected at an S/N>100 with Effelsberg. The two brightest bursts (B1 & B2) are shown in Figure 2 as waterfall plots. We combined all sub-bands of the UBB receiver where significant emission of the burst was detected. For burst B1 and B3, this corresponds to sub-band 1 and 2, while B2 shows significant emission in sub-bands 3 and 4.

[1] `https://indico.narit.or.th/event/197/page/654-tnro-40-m-tnrt`

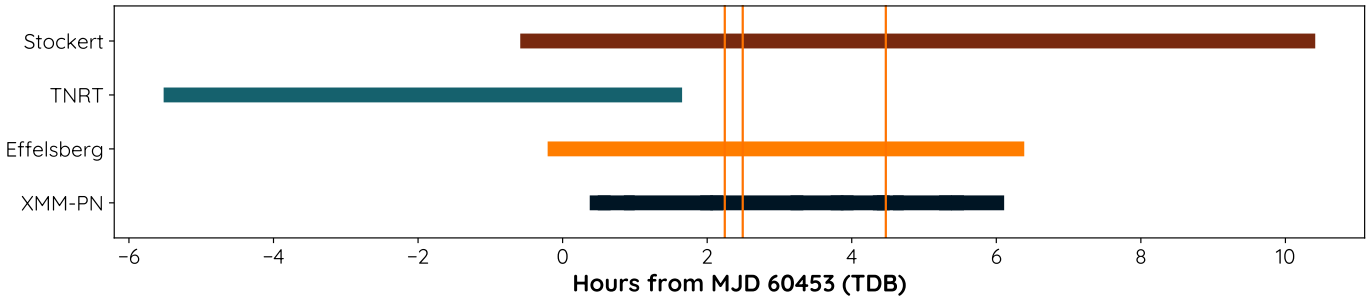

Fig. 1: Overview of the observing times (barycentric) and participating telescopes on 23 May 2024. For *XMM-Newton*-PN, the displayed time range corresponds to the GTIs. The three vertical lines indicate the arrival times of burst B1, B2 and B3 detected with Effelsberg.

Burst B1 shows temporal sub-structure, divided into three sub-bursts that seem to follow the typical sad-trombone scheme (e.g., Katz 2023). Bursts B2 and B3 are single bursts without visible sub-components. To calculate the fluence of each burst, we first averaged the flux density over the observing bandwidth, excluding RFI-flagged channels and then integrated the flux density over a 40 ms window centered on the burst arrival time. The resulting fluences are shown in Table 1. In order to compare the fluences derived from different observing bandwidths, we integrated it over the observing bandwidth (excluding RFI-flagged channels). This quantity is much more useful to compare the energy release of the burst with multi-wavelength observations, since it is independent of the bandwidth that was used to calculate the fluence. This bandwidth-integrated fluence is usually referred to as the "radio burst fluence" $\mathcal{F}_{\rm R}$ (e.g. Pearlman et al. 2023; Cook et al. 2024). By using the known redshift of the host galaxy of FRB 20240114A ($z = 0.13$, Bhardwaj et al. 2024) and assuming a flat Lambda-CDM model (Planck Collaboration et al. 2020), we calculated the intrinsic radio burst release energy $\rm E_R$ for every burst, following Zhang (2018). The obtained values are displayed in Table 1. The brightest burst in our observations, B1, summed over all three sub-components, exhibits a radio burst fluence $\mathcal{F}_{\rm R,B1} = 2.6 \times 10^{-17}\,\rm erg\,cm^{-2}$, which translates to a total release energy $\rm E_{R,B1} = 1.1 \times 10^{39}$erg. Note that all of these values can be understood as lower limits, since parts of the burst emission exceed the receiver bandwidth (at least for B1) and multiple channels within the burst bandwidth needed to be flagged due to RFI and could therefore not be considered for the fluence calculation.

3.2. X-ray burst emission

We checked the non-background corrected PN-event list (0.2−12 keV) for X-ray photons at the times of the detected radio bursts B1−B3. We used an extraction region with radius 0.01° (i.e., 90 % encircled energy fraction at 1.5 keV) centered on the position of FRB 20240114A determined by Snelders et al. (2024). The average background count rate in this region is $\sim 3 \times 10^{-2}$ cps. For burst B1, the closest X-ray photon after the burst was detected 48 s after the radio emission, for Burst B2 50 s and for Burst B3 17 s after the radio emission. This is consistent with the expected background rate, hence, we conclude that all three bursts are not detected at X-ray energies.

In order to derive an upper limit to the burst X-ray flux for each of the radio bursts, we used a similar method as described by Cook et al. (2024). We estimate the background rate at the position of FRB 20240114A using a 200 s window centered on the time of arrival of the burst. By applying low-count photon statistics using the `pwkit` library (Williams et al. 2017), following Kraft et al. (1991), we derive a $3\,\sigma$ (i.e., 99.73 % one-sided confidence level) upper limit of 5.9 photons at the time of the radio burst, or 6.5 photons when correcting for the encircled energy fraction. Considering a typical duration of magnetar-associated X-ray bursts of ∼100 ms as seen in SGR 1935+2154 (Mereghetti et al. 2020), a cutoff power law spectrum ($\Gamma = 1.56$, cutoff 84 keV) as observed in SGR 1935+2154 (Li et al. 2021) and an average hydrogen column density $N_{\rm H} = 5.0 \times 10^{20}\,\rm cm^{-2}$ in the direction of FRB 20240114A (HI4PI Collaboration et al. 2016), this translates to a $3\,\sigma$ upper limit to the unabsorbed X-ray fluence of $\mathcal{F}_{\rm X} < 3.4 \times 10^{-11}\,\rm erg\,cm^{-2}$ in the 0.2−12 keV band (following Appendix A of Tubín-Arenas et al. 2024). The corresponding upper limit to the intrinsic total X-ray energy release is $\rm E_X < 1.5 \times 10^{45}$ erg (0.2−12 keV). Assuming a more conservative 10 keV black-body spectrum ~~(cf.,~~ Cook et al. 2024), the $3\,\sigma$ upper limit to the unabsorbed X-ray fluence is $\mathcal{F}_{\rm X} < 1.7 \times 10^{-10}\,\rm erg\,cm^{-2}$ ($\rm E_X < 7.2 \times 10^{45}$ erg) in the 0.2−12 keV band.

We used the ~~calculated~~ radio burst fluences $\mathcal{F}_{\rm R}$ and the upper limit to the X-ray burst fluence $\mathcal{F}_{\rm X}$ to calculate upper limits on the X-ray-to-radio fluence ratio $\eta_{\rm x/r} = \mathcal{F}_{\rm X}/\mathcal{F}_{\rm R}$. Note that this fluence ratio always corresponds to specific observing bandwidths in the radio and X-ray. The fluence ratios for the three brightest bursts in our observing campaign are shown in Table 1. The most constraining limit can be obtained from burst B1, yielding a fluence ratio $\eta_{\rm x/r} < 1.3 \times 10^6$ at $3\,\sigma$ confidence, assuming a spectrum similar to SGR 1935+2154. The more conservative 10 keV black-body spectrum assumption leads to $\eta_{x/r} < 6.5 \times 10^6$.

3.3. Persistent X-ray emission

To determine the persistent X-ray flux from FRB 20240114A, we selected events coming from its position determined by Snelders et al. (2024) with a radius of 0.01° in an energy range of 0.2−12 keV. We defined background regions next to the position of the FRB without any X-ray sources to compare the number of collected photons at the position of the FRB with the background expectation. Using the method of Kraft et al. (1991) we calculate a $3\,\sigma$ upper limit to the persistent X-ray flux of FRB 20240114A from 57.3 ks of GTI PN-data. We find a $3\,\sigma$ upper limit of $< 2.4 \times 10^{-3}$ cps, corrected for the encircled energy fraction. Assuming a power law spectrum with $\Gamma = 2$ and the same $N_{\rm H}$ as in 3.2, this corresponds to a persistent X-ray flux limit of $< 1.0 \times 10^{-14}\,\rm erg\,cm^{-2}\,s^{-1}$. This corresponds to an isotropic luminosity $\mathcal{L}_{\rm X} < 4.3 \times 10^{41}\,\rm erg\,s^{-1}$ (0.2−12 keV) and

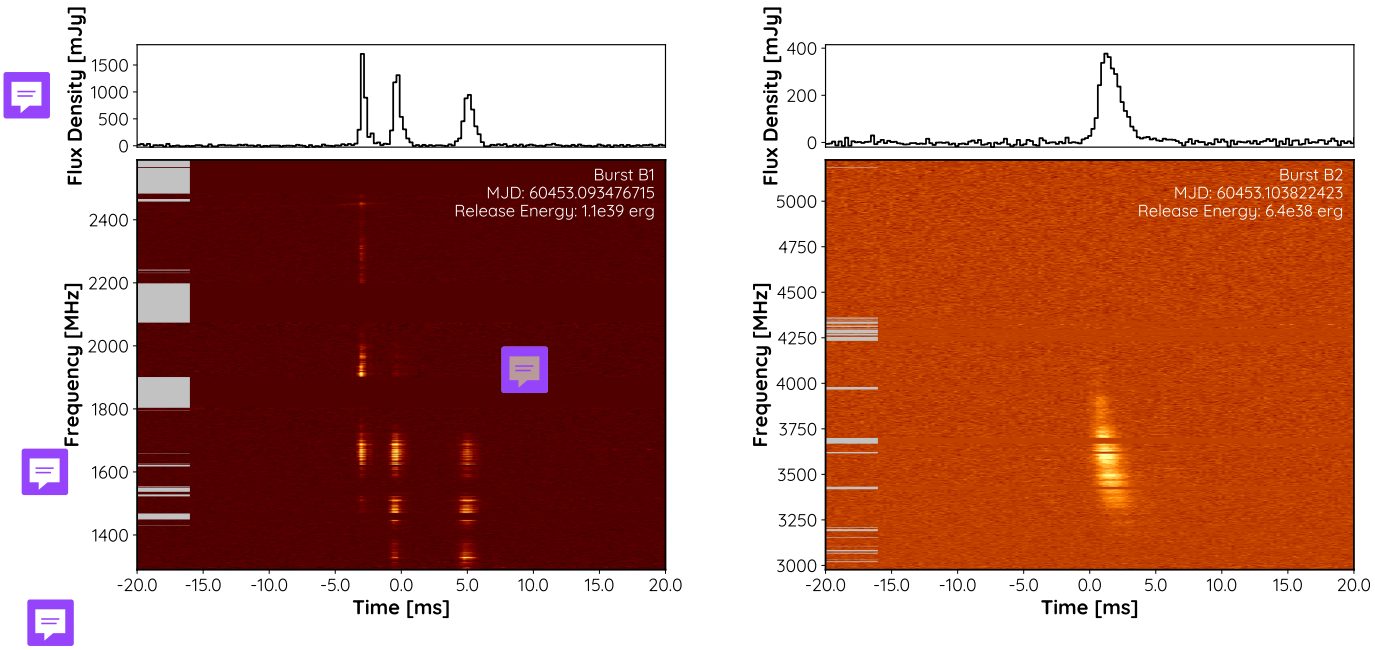

Fig. 2: Waterfall plots of two of the brightest bursts from FRB 20240114A that were detected simultaneous to the *XMM-Newton* observation on 23 May 2024 (left: B1, right: B2). RFI-flagged channels are highlighted by the light gray lines on the left. The top panel shows the flux density, averaged over the displayed bandwidth, excluding RFI-flagged channels. The displayed bandwidth for B1 (left) corresponds to the combined UBB sub-bands 1 and 2, while B2 (right) is shown in UBB sub-bands 3 and 4. The displayed MJD is the time of arrival of the burst at the barycenter of the solar system corrected to infinite frequency.

improves the upper limits reported by Verrecchia et al. (2024) based on *Swift* observations by a factor of 10−100.

4. Discussion

4.1. Comparison with other multi-wavelength FRB studies

In this section, we compare our results to multi-wavelength observations of other FRB sources, mainly focusing on ~~the most recent publication by~~ Cook et al. (2024), which includes an overview of many previous studies. Note that in all previous studies, no significant X-ray emission (neither persistent nor burst-like) was found. Cook et al. (2024) use X-ray fluences and energies in the 0.5−10 keV band. We therefore convert the limits on the X-ray burst fluence and the persistent X-ray flux from section 3 to the 0.5−10 keV energy band. In this energy band, the upper limit to the X-ray burst fluence corresponds to 2.7×10^{-11} erg cm^{-2} (cutoff power law) or 1.1×10^{-10} erg cm^{-2} (black-body spectrum), assuming the same spectral models as in section 3.

For the single burst X-ray fluence limits at the time of the radio bursts, we used a similar analysis as presented by Cook et al. (2024). ~~The upper limits derived by Cook et al. (2024)~~ are higher by ~ 35 % for the black-body spectrum scenario, which can be explained by the different assumed $N_{\rm H}$ values. While Cook et al. (2024) use a conservative value of $N_{\rm H} = 10^{22}$ cm^{-2}, trying to account for absorption at the source, we use the average hydrogen column density of $N_{\rm H} = 5.0 \times 10^{20}$ cm^{-2} in the direction of FRB 20240114A (HI4PI Collaboration et al. 2016). Assuming the more conservative value of $N_{\rm H} = 10^{22}$ cm^{-2}, our upper limit to the single burst X-ray fluence increases to 1.2×10^{-10} erg cm^{-2} for a black-body spectral model (0.5−10 keV). This value is still slightly lower as ~~the~~ limit obtained by Cook et al. (2024), which is likely due to the fact that we initially extracted a larger energy band of 0.2−12 keV from the *XMM-Newton* data and then down sampled to the 0.5−10 keV band. Moreover, it is unclear if Cook et al. (2024) used the same count-to-flux conversion based on Tubín-Arenas et al. (2024).

According to Cook et al. (2024), the most constraining fluence ratio limit for a single fast radio burst to date was found at $\eta_{\rm x/r} < 7 \times 10^6$ for FRB 20220912A (0.5−10 keV), assuming a 10 keV black-body X-ray spectrum. Our best limit obtained from the brightest burst B1 ($\eta_{\rm x/r} < 1.3 \times 10^6$) is significantly lower than this, but considers a different X-ray energy band (0.2−12 keV), different spectral model (cutoff power law) and different absorption. The assumption of a black-body spectrum seems very conservative, given that it is quite reasonable to assume a cutoff power law based on the observed X-ray emission of the Galactic magnetar SGR 1935+2154 (Li et al. 2021).

In the most conservative scenario (black-body, $N_{\rm H} = 10^{22}$ cm^{-2}) the limit from burst B1 transforms to $\eta_{\rm x/r} < 4.6 \times 10^6$ in the 0.5−10 keV band. This is still lower than any previously reported fluence ratio limit for a single burst, which is due to the fact that the radio bursts detected in our observation are more energetic than in previous multi-wavelength studies. The limit can be further constrained by applying the ~~novel~~ stacking approach introduced by Cook et al. (2024), however this requires accurate flux calibration of all 459 bursts detected within our campaign and will be done in a separate publication.

4.2. Constraints on FRB production mechanisms

While the upper limit to the X-ray-to-radio fluence ratio for burst B1 is the lowest one obtained so far for a single burst, it cannot rule out the currently favored FRB production models, based on magnetars. As pointed out by Cook et al. (2024), most

Table 1: Overview of the three brightest bursts detected within our multi-wavelength campaign

Burst-ID	TOA[a] [MJD]	Fluence[b] [Jy ms]	Bandwidth[c] [MHz]	Radio Burst[d] Fluence [erg cm^{-2}]	Radio Burst[e] Energy [erg]	X-ray Burst[f] Fluence [erg cm^{-2}]	Fluence Ratio[g] $\eta_{x/r}$
B1	60453.093476715	2.88	886	2.6×10^{-17}	1.1×10^{39}	$< 3.4 \times 10^{-11}$	$< 1.3 \times 10^{6}$
B2	60453.103822423	0.76	1992	1.5×10^{-17}	6.4×10^{38}	$< 3.4 \times 10^{-11}$	$< 2.3 \times 10^{6}$
B3	60453.186311511	1.52	835	1.3×10^{-17}	5.4×10^{38}	$< 3.4 \times 10^{-11}$	$< 2.6 \times 10^{6}$

[a] Time of arrival corrected to infinite frequency at the barycenter of the solar system. [b] Fluence averaged over the observing bandwidth. [c] Observing bandwidth used to calculate the average fluence, excludes flagged channels ~~within the band~~. [d] Radio burst fluence $\mathcal{F}_R$ (i.e., Fluence × Bandwidth). [e] Redshift corrected intrinsic total radio burst release energy. [f] Unabsorbed X-ray burst fluence $\mathcal{F}_X$ (0.2−12 keV), $3\,\sigma$ upper limit, assuming a cutoff power law spectrum as observed for SGR 1935+2154 (Li et al. 2021). [g] 3σ upper limit to the X-ray (0.2−12 keV) to radio fluence ratio ($\eta_{x/r} = \mathcal{F}_X/\mathcal{F}_R$).

magnetar-based models predict an X-ray-to-radio fluence ratio $\eta_{x/r} \approx 1 - 10^4$ (e.g., Margalit et al. 2020; Lu et al. 2020; Popov & Postnov 2010). Moreover, the X-ray-to-radio fluence ratio from the Galactic magnetar SGR 1935+2154 was observed to be $\eta_{x/r} \sim 2.5 \times 10^5$ (1−250 keV, Bochenek et al. 2020; CHIME/FRB Collaboration et al. 2020; Mereghetti et al. 2020; Li et al. 2021), which is still well below the most constraining upper limit for $\eta_{x/r}$ found for any extragalactic FRB. Corrected for typical *XMM-Newton* observing bands (0.2−12 keV), the expected $\eta_{x/r}$ from SGR 1935+2154 is even lower, by a factor of ∼ 3. Therefore, our observations are consistent with FRB 20240114A being powered by a magnetar, in agreement with synchrotron maser models ~~(e.g.~~ Metzger et al. 2019), and magnetospheric emission models ~~(e.g.,~~ Margalit et al. 2020; Lu et al. 2020; Zhong et al. 2024).

Given the extremely bright bursts from FRB 20240114A reported, ~~e.g.,~~ by (Shin & CHIME/FRB Collaboration 2024), and its hyperactivity, it is a prime target for future multi-wavelength studies. While future studies with current X-ray telescopes will not be able to place significantly lower limits on the X-ray flux, the detection of more energetic radio bursts up to a factor of 10−100 times brighter than found in our campaign are possible and would result in valuable constraints to $\eta_{x/r}$, reaching the value found for the Galactic magnetar SGR 1935+2154.

5. Conclusions & outlook

We observed the recently discovered repeating fast radio burst FRB 20240114A with the Effelsberg 100-m telescope, the Thai National Radio Telescope, the Astropeiler Stockert telescope and the X-ray satellite *XMM-Newton*. On 23 May 2024, we detected 459 radio bursts from FRB 20240114A using the Effelsberg UBB receiver, covering a frequency range from 1.3−6 GHz. In this work, we presented the three brightest bursts, detected at an S/N> 100 with Effelsberg. The brightest burst from this campaign (Burst B1, see Fig. 2) exhibits a radio burst fluence of 2.6×10^{-17} erg cm^{-2}. None of the bursts were detected with *XMM-Newton*, Stockert or TNRT. We used the *XMM-Newton* observations to derive upper fluence limits for associated X-ray bursts lasting 100 ms, which can be constrained to $\mathcal{F}_X < 3.4 \times 10^{-11}$ erg cm^{-2} in the 0.2−12 keV band at $3\,\sigma$ confidence. This corresponds to an X-ray-to-radio fluence ratio $\eta_{x/r} < 1.3 \times 10^6$ for the brightest burst. This is the lowest single burst limit to $\eta_{x/r}$ known to date. Considering different magnetar models for FRBs, ~~that~~ predict associated X-ray emission (~~e.g.~~ Metzger et al. 2019; Margalit et al. 2020; Lu et al. 2020; Zhong et al. 2024) this limit is consistent with FRB 20240114A being powered by a magnetar. Moreover, from the multi-wavelength detection of radio and X-ray bursts from the Galactic magnetar SGR 1935+2154, one expects $\eta_{x/r} \sim 2.5 \times 10^5$ (Bochenek et al. 2020; CHIME/FRB Collaboration et al. 2020; Mereghetti et al. 2020; Li et al. 2021), which is in agreement with our upper limit. That means FRB 20240114A could be powered by a similar mechanism as SGR 1935+2154. In a follow-up publication we are planning to stack all 459 bursts to derive an even lower limit to the X-ray/radio fluence ratio $\eta_{x/r}$ of FRB 20240114A, possibly challenging the value observed for the Galactic magnetar SGR 1935+2154. We like to emphasize that future multi-wavelength observations of highly energetic (~~i.e.,~~ high-fluence), extragalactic FRBs (e.g., Kirsten et al. 2024) have the potential to probe $\eta_{x/r}$ to even smaller values by a factor of 10−100, i.e., enabling the detection of X-ray burst emission in case of an emission mechanism similar to SGR 1935+2154.

Acknowledgements. We thank Amanda Cook for helpful discussions on the X-ray count-to-flux conversion. This work is based on observations with the 100-m telescope of the MPIfR (Max-Planck-Institut für Radioastronomie) at Effelsberg. FE and MK (M. Kadler) acknowledge support from the Deutsche Forschungsgemeinschaft (DFG, grant 447572188). MK (M. Krumpe) acknowledges support from the German Aerospace Center (DLR, grant FK2 50 OR 2307). LGS is a Lise Meitner research group leader and acknowledges support from the Max Planck Society. Based on observations obtained with XMM-Newton, an ESA science mission with instruments and contributions directly funded by ESA Member States and NASA. Partially of this research is based on observations made with the 40-m Thai National Radio Telescope at the Thai National Radio Astronomy Observatory under the open-use program ID ToO1 (Target of Opportunity 1), which is operated by the National Astronomical Research Institute of Thailand (Public Organization).

References

Agarwal, D. & Aggarwal, K. 2020, devanshkv/fetch: Software release with the manuscript
Agarwal, D., Aggarwal, K., Burke-Spolaor, S., Lorimer, D. R., & Garver-Daniels, N. 2020, Monthly Notices of the Royal Astronomical Society
Barr, E. D., Bansod, A., Behrend, J., et al. 2023, in 2023 XXXVth General Assembly and Scientific Symposium of the International Union of Radio Science (URSI GASS), We–J01–PM3–4
Barr, E. D., Champion, D. J., Kramer, M., et al. 2013, MNRAS, 435, 2234
Bhardwaj, M., Kirichenko, A., & Gil de Paz, A. 2024, The Astronomer's Telegram, 16613, 1
Bochenek, C. D., Ravi, V., Belov, K. V., et al. 2020, Nature, 587, 59
CHIME/FRB Collaboration, Andersen, B. C., Bandura, K. M., et al. 2020, Nature, 587, 54
Cook, A. M., Scholz, P., Pearlman, A. B., et al. 2024, ApJ, 974, 170
Gabriel, C., Denby, M., Fyfe, D. J., et al. 2004, in Astronomical Society of the Pacific Conference Series, Vol. 314, Astronomical Data Analysis Software and Systems (ADASS) XIII, ed. F. Ochsenbein, M. G. Allen, & D. Egret, 759
Gaia Collaboration, Vallenari, A., Brown, A. G. A., et al. 2023, A&A, 674, A1
Hessels, J. W. T., Spitler, L. G., Seymour, A. D., et al. 2019, ApJ, 876, L23
Hewitt, D. M., Huang, J., Hessels, J. W. T., et al. 2024, The Astronomer's Telegram, 16597, 1
HI4PI Collaboration, Ben Bekhti, N., Flöer, L., et al. 2016, A&A, 594, A116
Jaroenjittichai, P., Sugiyama, K., Kramer, B. H., et al. 2022, arXiv e-prints, arXiv:2210.04926

Joshi, P., Medina, A., Earwicker, J. T., et al. 2024, The Astronomer's Telegram, 16599, 1
Katz, J. I. 2023, MNRAS, 518, 2015
Kirsten, F., Ould-Boukattine, O. S., Herrmann, W., et al. 2024, Nature Astronomy, 8, 337
Kraft, R. P., Burrows, D. N., & Nousek, J. A. 1991, ApJ, 374, 344
Kumar, A., Maan, Y., & Bhusare, Y. 2024, The Astronomer's Telegram, 16452, 1
Kurpas, J., Schwope, A. D., Pires, A. M., & Haberl, F. 2024, A&A, 683, A164
Li, C. K., Lin, L., Xiong, S. L., et al. 2021, Nature Astronomy, 5, 378
Limaye, P. & Spitler, L. 2024, The Astronomer's Telegram, 16620, 1
Lu, W., Kumar, P., & Zhang, B. 2020, MNRAS, 498, 1397
Luo, J., Ransom, S., Demorest, P., et al. 2021, ApJ, 911, 45
Margalit, B., Beniamini, P., Sridhar, N., & Metzger, B. D. 2020, ApJ, 899, L27
Men, Y. & Barr, E. 2024, A&A, 683, A183
Mereghetti, S., Savchenko, V., Ferrigno, C., et al. 2020, ApJ, 898, L29
Metzger, B. D., Margalit, B., & Sironi, L. 2019, MNRAS, 485, 4091
Morello, V., Barr, E. D., Cooper, S., et al. 2019, MNRAS, 483, 3673
Ould-Boukattine, O. S., Dijkema, T. J., Gawronski, M., et al. 2024a, The Astronomer's Telegram, 16565, 1
Ould-Boukattine, O. S., Hessels, J. W. T., Kirsten, F., et al. 2024b, The Astronomer's Telegram, 16432, 1
Panda, U., Bhattacharyya, S., Dudeja, C., Kudale, S., & Roy, J. 2024, The Astronomer's Telegram, 16494, 1
Pearlman, A. B., Scholz, P., Bethapudi, S., et al. 2023, arXiv e-prints, arXiv:2308.10930
Pelliciari, D., Geminardi, A., Bernardi, G., et al. 2024, The Astronomer's Telegram, 16547, 1
Perley, R. A. & Butler, B. J. 2017, ApJS, 230, 7
Pilia, M., Burgay, M., Possenti, A., et al. 2020, ApJ, 896, L40
Piro, L., Bruni, G., Troja, E., et al. 2021, A&A, 656, L15
Planck Collaboration, Aghanim, N., Akrami, Y., et al. 2020, A&A, 641, A6
Platts, E., Weltman, A., Walters, A., et al. 2019, Phys. Rep., 821, 1
Popov, S. B. & Postnov, K. A. 2010, in Evolution of Cosmic Objects through their Physical Activity, ed. H. A. Harutyunian, A. M. Mickaelian, & Y. Terzian, 129–132
Ransom, S. 2011, PRESTO: PulsaR Exploration and Search TOolkit, Astrophysics Source Code Library, record ascl:1107.017
Ridnaia, A., Svinkin, D., Frederiks, D., et al. 2021, Nature Astronomy, 5, 372
Scholz, P., Bogdanov, S., Hessels, J. W. T., et al. 2017, ApJ, 846, 80
Scholz, P., Cook, A., Cruces, M., et al. 2020, ApJ, 901, 165
Scholz, P., Spitler, L. G., Hessels, J. W. T., et al. 2016, ApJ, 833, 177
Seymour, A., Michilli, D., & Pleunis, Z. 2019, DM_phase: Algorithm for correcting dispersion of radio signals, Astrophysics Source Code Library, record ascl:1910.004
Shin, K. & CHIME/FRB Collaboration. 2024, The Astronomer's Telegram, 16420, 1
Snelders, M. P., Bhandari, S., Kirsten, F., et al. 2024, The Astronomer's Telegram, 16542, 1
Spitler, L. G., Cordes, J. M., Chatterjee, S., & Stone, J. 2012, The Astrophysical Journal, 748, 73
Tavani, M., Casentini, C., Ursi, A., et al. 2021, Nature Astronomy, 5, 401
Tian, J., Rajwade, K. M., Pastor-Marazuela, I., et al. 2024, MNRAS, 533, 3174
Trudu, M., Pilia, M., Nicastro, L., et al. 2023, A&A, 676, A17
Tubín-Arenas, D., Krumpe, M., Lamer, G., et al. 2024, A&A, 682, A35
Uttarkar, P. A., Kumar, P., Lower, M. E., & Shannon, R. M. 2024, The Astronomer's Telegram, 16430, 1
van Straten, W. & Bailes, M. 2011, PASA, 28, 1
van Straten, W., Demorest, P., & Oslowski, S. 2012, Astronomical Research and Technology, 9, 237
Verrecchia, F., Perri, M., Tavani, M., et al. 2024, The Astronomer's Telegram, 16645, 1
Williams, P. K. G., Clavel, M., Newton, E., & Ryzhkov, D. 2017, pwkit: Astronomical utilities in Python, Astrophysics Source Code Library, record ascl:1704.001
Yan, Z., Yu, W., Page, K. L., et al. 2024, arXiv e-prints, arXiv:2402.12084
Zhang, B. 2018, ApJ, 867, L21
Zhang, J., Wu, Q., Cao, S., et al. 2024a, The Astronomer's Telegram, 16505, 1
Zhang, J., Zhu, Y., Cao, S., et al. 2024b, The Astronomer's Telegram, 16433, 1
Zhong, S.-Q., Li, L., Zhang, B., & Dai, Z.-G. 2024, ApJ, 976, 52

Appendix A: Effelsberg UBB data analysis

The UBB receiver delivers `psrfits` files for every sub-band, which were searched for single bursts using `TransientX` (Men & Barr 2024) separately in every sub-band. We performed a search for short bursts with a maximum width of 10 ms on the full resolution data from the UBB. Additionally, we ran a search for longer bursts with a maximum width of 100 ms with a time down sampling factor of 10. The detected candidates were filtered using the `replot_fil` command within `TransientX` using an S/N cutoff of 7 and then inspected manually to identify false positive detections. We corrected the arrival times from the different bands to infinite frequency and matched any overlapping candidates to avoid duplication of the same burst detected in multiple bands. We extracted 1 s pulsar archive snippets around the burst arrival times using `DSPSR` (van Straten & Bailes 2011). Flux and polarization calibration was performed using the `pac` and `fluxcal` tasks within `PSRCHIVE` (van Straten et al. 2012) for every sub-band separately. Calibration solutions were derived from observations of 3C 48 on 9 May 2024 using the Perley & Butler (2017) flux scale. To be conservative, we assume a 5 % error on the flux scale, which is on the high-end of the suggested error by Perley & Butler (2017). Prior to flux calibration, automatic radio frequency interference (RFI) cleaning was performed on the archive files using `clfd` (Morello et al. 2019), as well as additional manual flagging using the `PSRCHIVE` tool `pazi`. To combine the different sub-bands files from the UBB we loaded the calibrated and RFI-flagged archive files into the `PSRCHIVE` python framework and combined them as `numpy` arrays. Our code to combine the different sub-bands of the UBB is available on GitHub[2].

For further analysis, we dedispersed all bursts using a common DM value of $(527.979 \pm 0.085)\,\mathrm{pc\,cm^{-3}}$. This DM value was derived from burst B1, which shows the most complex temporal substructure among the three brightest bursts, using the `DM_PHASE` package (Seymour et al. 2019). We assume that the DM of FRB 20240114A does not vary significantly within the observation duration, which is valid for other repeating FRBs (e.g., Hessels et al. 2019). In a follow-up study, we will address this question for FRB 20240114A in more detail and study possible DM variations between the 459 detected bursts. The topocentric arrival times of the bursts were corrected to infinite frequency and to the arrival time at the barycenter of the solar system using `PINT` (Luo et al. 2021). We note that the uncertainty of the DM and the exact position of the FRB can introduce an error on the order of several milliseconds.

Appendix B: Astrometric Correction for XMM-Newton data

In order to determine the exact position of FRB 20240114A in the *XMM-Newton* images, we performed a source detection in the full PN and MOS data of every observation using the `edetect_stack` task in `SAS`. While there is no significant source detected in the small-window region of the chips, the outer regions of the MOS-chip still allow for the detection of several field sources. The detected X-ray sources were matched with the Gaia DR3 catalog (Gaia Collaboration et al. 2023) using `eposcorr`, as described by Kurpas et al. (2024). The resulting astrometric corrections in Right Ascension ΔRA and in declination ΔDec are shown in Table B.1 and were applied to each dataset. The corrections are small compared to the extraction radius. In order to test if they lead to a significant change in our results, we performed all of our analysis also without applying this correction, which indeed has no significant effect on the results since the corrections are small compared to the PSF.

Table B.1: Astrometric corrections for the *XMM-Newton* pointings calculated with `eposcorr`.

Obs.ID	ΔRA ["]	ΔDec ["]
0935190601	1.08 ± 0.11	0.58 ± 0.17
0935190701	-0.115 ± 0.021	0.555 ± 0.060
0935191001	1.6195 ± 0.0039	0.740 ± 0.025

[2] `https://github.com/flep198/ubb_tools`